DEUTSCHES ELEKTRONEN-SYNCHROTRON
Ein Forschungszentrum der Helmholtz-Gemeinschaft

DESY 20-047
IFT-UAM/CSIC-20-041
arXiv:2003.05422
March 2020

The "96 GeV Excess" at the LHC

T. Biekötter

Deutsches Elektronen-Synchrotron DESY, Hamburg

M. Chakraborti

IFT (UAM/CSIC), Universidad Autónoma de Madrid, Cantoblanco, Spain

S. Heinemeyer

IFT (UAM/CSIC), Universidad Autónoma de Madrid, Cantoblanco, Spain

and

Campus of International Excellence UAM+CSIC,
Cantoblanco, Madrid, Spain

and

Instituto de Física de Cantabria (CSIC-UC), Santander, Spain

ISSN 0418-9833

NOTKESTRASSE 85 - 22607 HAMBURG

IFT–UAM/CSIC–20-041 [a]
DESY 20–047

The "96 GeV excess" at the LHC

T. Biekötter
DESY, Notkestrasse 85, D-22607 Hamburg, Germany

M. Chakraborti
IFT (UAM/CSIC), Universidad Autónoma de Madrid, Cantoblanco, E-28048, Spain

S. Heinemeyer
IFT (UAM/CSIC), Universidad Autónoma de Madrid Cantoblanco, E-28048, Spain
Campus of International Excellence UAM+CSIC, Cantoblanco, E-28049, Madrid, Spain
Instituto de Física de Cantabria (CSIC-UC), E-39005 Santander, Spain

The CMS collaboration reported an intriguing $\sim 3\,\sigma$ (local) excess at 96 GeV in the light Higgs-boson search in the diphoton decay mode. This mass coincides with a $\sim 2\,\sigma$ (local) excess in the $b\bar{b}$ final state at LEP. We briefly review the proposed combined interpretations for the two excesses. In more detail we review the interpretation of this possible signal as the lightest Higgs boson in the 2 Higgs Doublet Model with an additional real Higgs singlet (N2HDM). We show which channels have the best prospects for the discovery of additional Higgs bosons at the upcoming Run 3 of the LHC.

1 Introduction

The Higgs boson discovered in 2012 by ATLAS and CMS [1, 2] is so far consistent with the existence of a Standard-Model (SM) Higgs boson [3] with a mass of $\sim 125\,\text{GeV}$. However, the experimental uncertainties on the Higgs-boson couplings are (if measured already) at the precision of $\sim 20\%$, so that there is room for Beyond Standard-Model (BSM) interpretations. Many theoretically well motivated extensions of the SM contain additional Higgs bosons. In particular, the presence of Higgs bosons lighter than 125 GeV is still possible.

Searches for light Higgs bosons have been performed at LEP, the Tevatron and the LHC. Besides the SM-like Higgs boson at 125 GeV no further detections of scalar particles have been reported. However, two excesses have been seen at LEP and the LHC at roughly the same mass, hinting to a common origin of both excesses via a new particle state. LEP observed a $2.3\,\sigma$ local excess in the $e^+e^- \to Z(H \to b\bar{b})$ searches [4], consistent with a scalar of mass $\sim 98\,\text{GeV}$, where the mass resolution is rather imprecise due to the hadronic final state. The signal strength was extracted to be $\mu_{\text{LEP}} = 0.117 \pm 0.057$. The signal strength μ_{LEP} is the measured cross section normalized to the SM expectation assuming a SM Higgs-boson mass at the same mass.

CMS searched for light Higgs bosons in the diphoton final state. Run II [5] results show a local excess of $\sim 3\,\sigma$ at $\sim 96\,\text{GeV}$, and a similar excess of $2\,\sigma$ at roughly the same mass [6] in Run I. Assuming dominant gluon fusion production the excess corresponds to $\mu_{\text{CMS}} = 0.6 \pm 0.2$. First Run II results from ATLAS with $80\,\text{fb}^{-1}$ in the diphoton final state turned out to be weaker than the corresponding CMS results, see, e.g., Fig. 1 in [7].

Here we first briefly review the models that have been proposed to explain the two excesses together. Then we concentrate on the 2 Higgs Doublet Model with an additional real Higgs singlet (N2HDM). It is shown that the type II and type IV (flipped) of the N2HDM can perfectly accommodate both excesses simultaneously, while being in agreement with all experimental and theoretical constraints. The excesses are most easily accommodated in the type II N2HDM,

[a] Talk presented at the IAS Program on High Energy Physics (HEP) 2020.

which resembles the Yukawa structure of supersymmetric models. We show which channels have the best prospects for the discovery of additional Higgs bosons at the upcoming Run 3 of the LHC. This complements our original N2HDM analysis [8], together with previous proceedings extending the original work with additional ILC/LHC/EWPO analyses [9], as well as e^+e^-/ILC specific analyses [10].

2 The experimental data and possible BSM interpretations

LEP reported a $2.3\,\sigma$ local excess in the $e^+e^- \to Z(H \to b\bar{b})$ searches [4], which would be consistent with a scalar mass of $\sim$ 98 GeV (but due to the final state the mass resolution is rather coarse). The "excess" corresponds to

$$\mu_{\rm LEP} = \frac{\sigma\left(e^+e^- \to Z\phi \to Zb\bar{b}\right)}{\sigma^{SM}\left(e^+e^- \to ZH_{\rm SM} \to Zb\bar{b}\right)} = 0.117 \pm 0.057\ , \tag{1}$$

where the signal strength $\mu_{\rm LEP}$ is the measured cross section normalized to the SM expectation, with the SM Higgs-boson mass at $\sim$ 98 GeV. The value for $\mu_{\rm LEP}$ was extracted in [11] using methods described in [12].

CMS Run II searches for Higgs bosons decaying in the diphoton final state show a local excess of $\sim 3\,\sigma$ around $\sim$ 96 GeV [13], with a similar excess of $2\,\sigma$ in the Run I data at a comparable mass. In this case the "excess" corresponds to (combining 7, 8 and 13 TeV data)

$$\mu_{\rm CMS} = \frac{\sigma\left(gg \to \phi \to \gamma\gamma\right)}{\sigma^{\rm SM}\left(gg \to H_{\rm SM} \to \gamma\gamma\right)} = 0.6 \pm 0.2\ . \tag{2}$$

First Run II results from ATLAS with $80\,{\rm fb}^{-1}$ in the $\gamma\gamma$ searches below 125 GeV were published [14]. While no significant excess above the SM expectation was observed in the mass range between 65 and 110 GeV, it was found that the limit on cross section times branching ratio obtained in the diphoton final state by ATLAS is not only well above $\mu_{\rm CMS}$, but even weaker than the corresponding upper limit obtained by CMS at $\sim$ 96 GeV [7] (see Fig. 1 therein).

Several analyses attempted to explain the *combined* "excess" of LEP and CMS in a variety of BSM models[b]. To our knowledge explanations exist in the following frameworks (see also [7,15,16]):

- Higgs singlet with additional vector-like matter, as well as Type-I 2HDM [17].
- Radion model [18].
- Type-I 2HDM with a moderately-to-strongly fermiophobic CP-even Higgs [19].
- $\mu\nu$SSM with one [20] and three generations [21] of right-handed neutrinos.
- Higgs associated with the breakdown of an $U(1)_{L_\mu L_\tau}$ symmetry [22].
- Various realizations of the NMSSM [23,24].
- Higgs inflation inspired μNMSSM [25].
- NMSSM with a seesaw extension [26].
- N2HDM [8], as will be discussed below.
- Minimal dilaton model [27].

[b] More analyses attempted to explain one of the two "excesses", but we will not discuss these further here.

- SM extended by a complex singlet scalar field (which can also accommodate a pseudo-Nambu Goldstone dark matter) [28].[c]
- Composite framework containing a pseudo-Nambu Goldstone-type light scalar [16].
- Anomaly-free $U(1)'$ extensions of SM with two complex scalar singlets [29].[c]

On the other hand, in the MSSM the CMS excess cannot be realized [30].

3 The N2HDM analysis

We discussed in [8] how a $\sim 96\,\text{GeV}$ Higgs boson of the Next to minimal 2 Higgs Doublet Model (N2HDM) [31, 32] can be the origin of both excesses in the type II and type IV scenarios. The N2HDM extends the CP-conserving 2 Higgs Doublet Model (2HDM) by a real scalar singlet field. In analogy to the 2HDM, a Z_2 symmetry is imposed to avoid flavor changing neutral currents at the tree level, which is only softly broken in the Higgs potential. Furthermore, a second Z_2 symmetry, under which the singlet field changes the sign, constraints the scalar potential. This symmetry is broken spontaneously as soon as the singlet field obtains a vacuum expectation value (vev).

In total, the Higgs sector of the N2HDM consists of 3 CP-even Higgs bosons h_i, 1 CP-odd Higgs boson A, and 2 charged Higgs bosons $H^{\pm}$. In principle, each of the particles h_i can account for the SM Higgs boson at 125 GeV. In our analysis, h_2 will be identified with the SM Higgs boson, while h_1 plays the role of the potential state at $\sim 96\,\text{GeV}$. The third CP-even and the CP-odd states h_3 and A were assumed to be heavier than 400 GeV to avoid LHC constraints. The charged Higgs-boson mass was set to be larger than 650 GeV to satisfy constraints from flavor physics observables.

In the physical basis the 12 independent parameters of the model are the mixing angles in the CP-even sector $\alpha_{1,2,3}$, the ratio of the vevs of the Higgs doublets $\tan\beta = v_2/v_1$, the SM vev $v = \sqrt{v_1^2 + v_2^2}$, the vev of the singlet field v_S, the masses of the physical Higgs bosons $m_{h_{1,2,3}}$, m_A and $M_{H^{\pm}}$, and the soft Z_2 breaking parameter m_{12}^2. Using the public code `ScannerS` [32, 33] we performed a scan over the following parameter ranges:

$$\begin{aligned} 95 \text{ GeV} \leq m_{h_1} \leq 98 \text{ GeV} \,, \quad m_{h_2} = 125.09 \text{ GeV} \,, \quad 400 \text{ GeV} \leq m_{h_3} \leq 1000 \text{ GeV} \,, \\ 400 \text{ GeV} \leq m_A \leq 1000 \text{ GeV} \,, \quad 650 \text{ GeV} \leq M_{H^{\pm}} \leq 1000 \text{ GeV} \,, \\ 0.5 \leq \tan\beta \leq 4 \,, \quad 0 \leq m_{12}^2 \leq 10^6 \text{ GeV}^2 \,, \quad 100 \text{ GeV} \leq v_S \leq 1500 \text{ GeV} \,. \end{aligned} \tag{3}$$

The following experimental and theoretical constraints were taken into account:
- tree-level perturbativity, boundedness-from-below and global-minimum conditions
- Cross-section limits from collider searches using `HiggsBounds v.5.3.2` [34–37]
- Signal-strength measurements of the SM Higgs boson using `HiggsSignals v.2.2.3` [38–40]
- Various flavor physics observables, in particular excluding $M_{H^{\pm}} < 650$ GeV for all values of $\tan\beta$ in the type II and IV.
- Electroweak precision observables in terms of the oblique parameters S, T and U [41, 42]

For more details we refer to [8]. The relevant input for `HiggsBounds` and `HiggsSignals`, (decay withs, cross sections), were obtained using the public codes `N2HDECAY` [32, 43] and `SusHi` [44, 45].

The results of our parameter scans in the type II and type IV N2HDM, as given in [8], show that both types of the N2HDM can accommodate the excesses simultaneously, while being in agreement with all considered constraints described above. A preference of larger values of μ_{CMS} in the type II scenario is visible, which is caused by the suppression of decays into τ-pairs (see [8] for details).

[c] It should be noted that in this model the required di-photon decay rate is reached by adding additional charged particles, coupling to the 96 GeV scalar.

4 Prospects for the LHC Run 3

As was shown in [8, 9], the searches for additional N2HDM Higgs bosons place important constraints on the allowed parameter space. As discussed above, we employ the code `HiggsBounds v.5.3.2` [34–37] to apply these searches to the N2HDM parameter space. For each parameter point `HiggsBounds` performs the following test. For each Higgs boson in the model `HiggsBounds` determines the search channel with the potentially highest sensitivity by comparing the model prediction with the *expected* limit. Subsequently, only this channel is used to test the BSM Higgs boson using the *observed* limit on cross section times branching ratio at the 95% CL. If the ratio

$$r := \frac{\sigma \times \mathrm{BR(predicted)}}{\sigma \times \mathrm{BR(observed\ limit)}} \tag{4}$$

is found to be larger ≥ 1, the parameter point is considered excluded at the 95% CL.

Conversely, points with $r < 1$ are not excluded. In general, points with r below, but close to 1 might be tested in the next round of experimental data. This is only a rough estimate, since values of r close to 1 may also be caused by a downward fluctuation of the background. Nevertheless, we regard points with

$$0.8 \leq r < 1.0 \tag{5}$$

as having good chances to be tested in the next round of experimental analyses.

In Fig. 1 we show exactly these points corresponding to Eq. 5 of our type II parameter scan, focusing on the LHC prospects (i.e. disregarding the LEP searches). The upper, middle and lower plot show the planes of $M_{H^\pm}$-$\tan\beta$, m_{h_3}-m_A and $|\alpha_1|$-$|\alpha_2|$, respectively. The color coding denotes the corresponding Higgs boson and its most senstive search channel. One can identify two main search channels:

- $pp \to H^\pm tb \to (tb)tb$
- $pp \to h_3 \to ZZ \to 4\mathrm{f}$

A third channel, $pp \to h_2 q\bar{q} \to (W^+W^-)q\bar{q}$, plays only a minor role and will not be discussed further.

In the upper plot of Fig. 1, showing the results in the $M_{H^\pm}$-$\tan\beta$ plane, one can see that the charged Higgs-boson channel is relevant at the lowest $M_{H^\pm}$ values, $M_{H^\pm} \leq 710$ GeV, and at the lowest $\tan\beta$ values, $\tan\beta \leq 1.05$. This region partially overlaps with exclusions from flavour physics observables, which are the origin of the sharp edge of points for even smaller values of $\tan\beta$. The parameter space that can be tested with the heavy neutral Higgs production covers roughly the triangle up to $M_{H^\pm} \leq 820$ GeV and $\tan\beta \leq 1.3$. However, while this parameter space does offer interesting possibilities for future heavy Higgs-boson searches at the LHC, it should be kept in mind that there are also points in this region with $r < 0.8$ and correspondingly weaker discovery potential. A detailed analysis of the (HL-)LHC prospects for the heavy (neutral and charged) Higgs-boson dicovery in the above denoted channels would be desirable.

The middle plot of Fig. 1 shows the m_{h_3}-m_A plane, following the general pattern based on the analysis of electroweak precision observables, mainly the T parameter [9]. One can observe an approximate separation of the heavy neutral Higgs-boson decay channels as a function of m_{h_3}. The searches for charged Higgs bosons, on the other hand, are widely distributed in the allowed parameter space. The bottom plot of Fig. 1, showing the results in the $|\alpha_1|$-$|\alpha_2|$ plane indicates a rather uniform distribution of the various Higgs-boson search channel, where the analysis combining all $h_3 \to ZZ$ decay channels is located at larger (smaller) values of $|\alpha_1|$ ($|\alpha_2|$). It should be noted that the upper limit on the $|\alpha_2|$ values is due to an upper limit on the possible singlet component of the 96 GeV scalar in our scans.

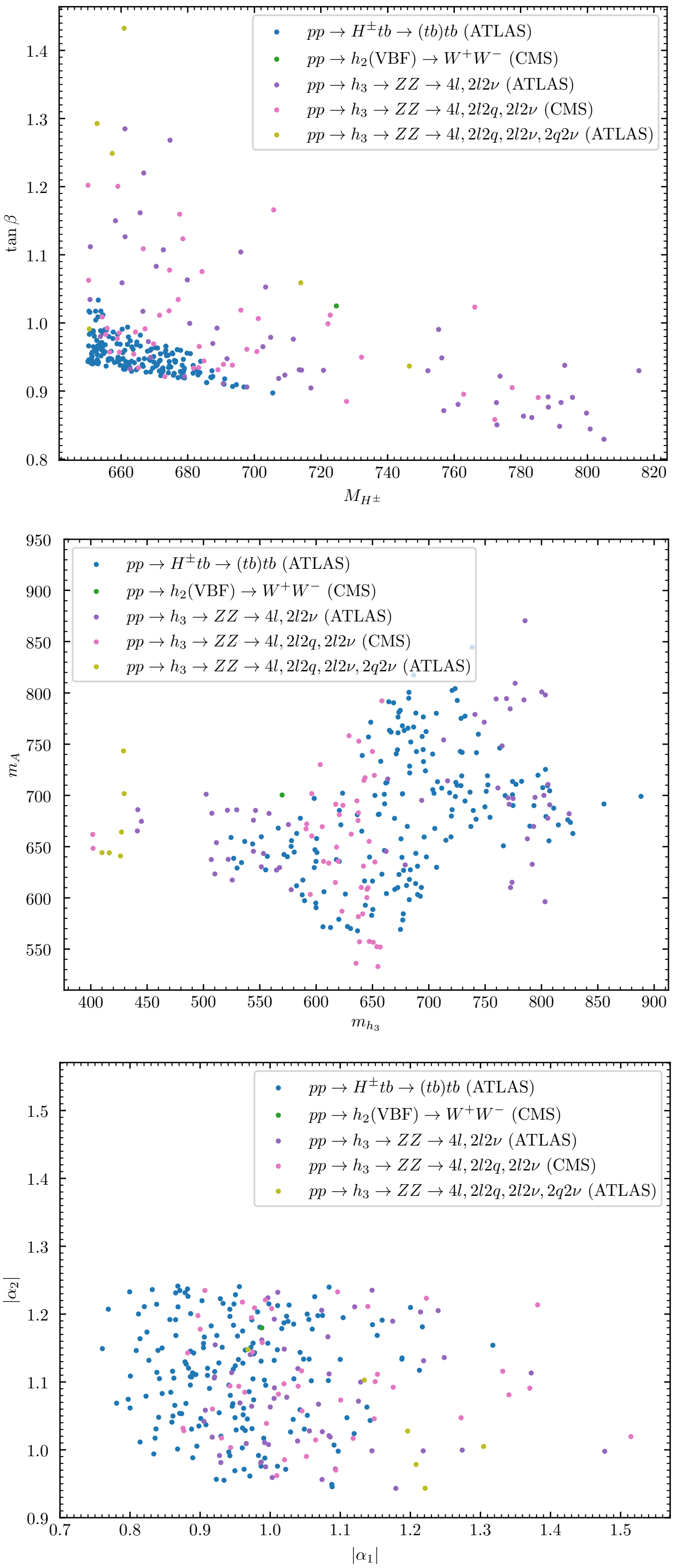

Figure 1 – Prospects for the discovery of additional Higgs bosons at the LHC Run 3 (see text). The upper, middle and lower plot show the planes of $M_{H^{\pm}}$-$\tan\beta$, m_{h_3}-m_A and $|\alpha_1|$-$|\alpha_2|$, respectively.

5 Conclusion

The possibility of the N2HDM explaining the CMS and the LEP excess simultaneously offers interesting prospects to be probed experimentally in the near future. Here we have focused on the possibilities to discover additional heavy Higgs bosons in the upcoming LHC runs. (Prospects for the coupling measurements of the 125 GeV Higgs boson at the HL-LHC and the ILC, as well as the direct production of the 96 GeV Higgs boson at the ILC can be found in [8, 10].) We find in particular that the searches for the charged Higgs bosons as well as for the heavy CP-even Higgs boson offer interesting prospects at the lower allowed values of $M_{H^\pm}$ and $\tan\beta$. A detailed analysis of the (HL-)LHC prospects for the heavy (neutral and charged) Higgs-boson dicovery in the above denoted channels would be highly desirable.

Acknowledgements

The work was supported in part by the MEINCOP (Spain) under contract FPA2016-78022-P and in part by the AEI through the grant IFT Centro de Excelencia Severo Ochoa SEV-2016-0597. The work of S.H. was supported in part by the Spanish Agencia Estatal de Investigación (AEI), in part by the EU Fondo Europeo de Desarrollo Regional (FEDER) through the project FPA2016-78645-P, in part by the "Spanish Red Consolider MultiDark" FPA2017-90566-REDC. T.B. is supported by the Deutsche Forschungsgemeinschaft under Germany's Excellence Strategy EXC2121 "Quantum Universe" - 390833306.

References

1. Georges Aad et al. *Phys. Lett.*, B716:1–29, 2012.
2. Serguei Chatrchyan et al. *Phys. Lett.*, B716:30–61, 2012.
3. Georges Aad et al. *JHEP*, 08:045, 2016.
4. R. Barate et al. *Phys. Lett.*, B565:61–75, 2003.
5. Albert M Sirunyan et al. arXiv:1811.08459.
6. Technical Report CMS-PAS-HIG-14-037, 2015.
7. S. Heinemeyer and T. Stefaniak. arXiv:1812.05864.
8. T. Biekotter, M. Chakraborti, and S. Heinemeyer. *Eur. Phys. J.*, C80(1):2, 2020.
9. T. Biekotter, M. Chakraborti, and S. Heinemeyer. In *31st Rencontres de Blois on Particle Physics and Cosmology Blois, France, June 2-7, 2019*, arXiv:1910.06858.
10. T. Biekotter, M. Chakraborti, and S. Heinemeyer. In *International Workshop on Future Linear Colliders (LCWS 2019) Sendai, Miyagi, Japan, October 28-November 1, 2019*, arXiv:2002.06904.
11. Junjie Cao, Xiaofei Guo, Yangle He, Peiwen Wu, and Yang Zhang. *Phys. Rev.*, D95(11):116001, 2017.
12. Aleksandr Azatov, Roberto Contino, and Jamison Galloway. *JHEP*, 04:127, 2012. [Erratum: JHEP04,140(2013)].
13. Technical Report CMS-PAS-HIG-17-013, CERN, 2017.
14. Technical Report ATLAS-CONF-2018-025, 2018.
15. S. Heinemeyer. *Int. J. Mod. Phys.*, A33(31):1844006, 2018.
16. Francois Richard. arXiv:2001.04770.
17. Patrick J. Fox and Neal Weiner. *JHEP*, 08:025, 2018.
18. Francois Richard. arXiv:1712.06410.
19. Ulrich Haisch and Augustinas Malinauskas. *JHEP*, 03:135, 2018.
20. T. Biekotter, S. Heinemeyer, and C. Munoz. *Eur. Phys. J.*, C78(6):504, 2018.
21. T. Biekotter, S. Heinemeyer, and C. Munoz. *Eur. Phys. J.*, C79(8):667, 2019.
22. Da Liu, Jia Liu, Carlos E. M. Wagner, and Xiao-Ping Wang. *JHEP*, 06:150, 2018.

23. F. Domingo, S. Heinemeyer, S. Paßehr, and G. Weiglein. *Eur. Phys. J.*, C78(11):942, 2018.
24. Kiwoon Choi, Sang Hui Im, Kwang Sik Jeong, and Chan Beom Park. *Eur. Phys. J.*, C79(11):956, 2019.
25. W. G. Hollik, S. Liebler, G. Moortgat-Pick, S. Paßehr, and G. Weiglein. *Eur. Phys. J.*, C79(1):75, 2019.
26. Junjie Cao, Xinglong Jia, Yuanfang Yue, Haijing Zhou, and Pengxuan Zhu. *Phys. Rev.*, D101(5):055008, 2020.
27. Lijia Liu, Haoxue Qiao, Kun Wang, and Jingya Zhu. *Chin. Phys.*, C43(2):023104, 2019.
28. James M. Cline and Takashi Toma. *Phys. Rev.*, D100(3):035023, 2019.
29. Juan Antonio Aguilar-Saavedra and Filipe Rafael Joaquim. arXiv:2002.07697.
30. P. Bechtle, H. E. Haber, S. Heinemeyer, O. Stål, T. Stefaniak, G. Weiglein, and L. Zeune. *Eur. Phys. J.*, C77(2):67, 2017.
31. Chien-Yi Chen, Michael Freid, and Marc Sher. *Phys. Rev.*, D89(7):075009, 2014.
32. M. Muhlleitner, M. O. P. Sampaio, R. Santos, and J. Wittbrodt. *JHEP*, 03:094, 2017.
33. Rita Coimbra, Marco O. P. Sampaio, and Rui Santos. *Eur. Phys. J.*, C73:2428, 2013.
34. P. Bechtle, O. Brein, S. Heinemeyer, G. Weiglein, and K. Williams. *Comput. Phys. Commun.*, 181:138–167, 2010.
35. P. Bechtle, O. Brein, S. Heinemeyer, G. Weiglein, and K. Williams. *Comput. Phys. Commun.*, 182:2605–2631, 2011.
36. P. Bechtle, O. Brein, S. Heinemeyer, O. Stål, T. Stefaniak, G. Weiglein, and K. Williams. *Eur. Phys. J.*, C74(3):2693, 2014.
37. P. Bechtle, S. Heinemeyer, O. Stål, T. Stefaniak, and G. Weiglein. *Eur. Phys. J.*, C75(9):421, 2015.
38. P. Bechtle, S. Heinemeyer, O. Stål, T. Stefaniak, and G. Weiglein. *Eur. Phys. J.*, C74(2):2711, 2014.
39. Oscar Stål and Tim Stefaniak. *PoS*, arXiv:1310.4039.
40. P. Bechtle, S. Heinemeyer, O. Stål, T. Stefaniak, and G. Weiglein. *JHEP*, 11:039, 2014.
41. Michael E. Peskin and Tatsu Takeuchi. *Phys. Rev. Lett.*, 65:964–967, 1990.
42. Michael E. Peskin and Tatsu Takeuchi. *Phys. Rev.*, D46:381–409, 1992.
43. A. Djouadi, J. Kalinowski, and M. Spira. *Comput. Phys. Commun.*, 108:56–74, 1998.
44. R. Harlander, S. Liebler, and H. Mantler. *Comput. Phys. Commun.*, 184:1605, 2013.
45. R. Harlander, S. Liebler, and H. Mantler. *Comput. Phys. Commun.*, 212:239, 2017.